November 2000

Polarized spectroscopy of aligned single-wall carbon nanotubes

J. Hwang
University of Florida

H. H. Gommans
University of Florida

A. Ugawa
University of Florida

H. Tashiro
University of Florida

Reto Haggenmueller
University of Pennsylvania

See next page for additional authors

Polarized spectroscopy of aligned single-wall carbon nanotubes

Abstract
Polarized resonant Raman and optical spectroscopy of aligned single-wall carbon nanotubes show that the optical transitions are strongly polarized along the nanotubes axis. This behavior is consistent with recent electronic structure calculations.

Author(s)
J. Hwang, H. H. Gommans, A. Ugawa, H. Tashiro, Reto Haggenmueller, Karen I. Winey, John E. Fischer, D. B. Tanner, and A. G. Rinzler

PHYSICAL REVIEW B VOLUME 62, NUMBER 20 15 NOVEMBER 2000-II

Polarized spectroscopy of aligned single-wall carbon nanotubes

J. Hwang,[1] H. H. Gommans,[1] A. Ugawa,[1] H. Tashiro,[1] R. Haggenmueller,[2] K. I. Winey,[2] J. E. Fischer,[2] D. B. Tanner,[1] and A. G. Rinzler[1]

[1]*Department of Physics, University of Florida, Gainesville, Florida 32611-8440*

[2]*Department of Materials Science, University of Pennsylvania, Philadelphia, Pennsylvania 19104*

(Received 15 August 2000; revised manuscript received 26 September 2000)

Polarized resonant Raman and optical spectroscopy of aligned single-wall carbon nanotubes show that the optical transitions are strongly polarized along the nanotubes axis. This behavior is consistent with recent electronic structure calculations.

Recently, unusual orientation-dependent behaviors were measured in polarized Raman spectroscopy on fibers of aligned single-wall carbon nanotubes (SWNT).[1,2] In particular, it was observed that for scattered light analyzed parallel to the incident laser polarization (VV geometry) all SWNT Raman peaks evidenced a dramatic decrease in intensity as the fiber orientation was rotated from parallel to perpendicular with respect to the incident polarization. This behavior is contrary to expectations based on the assigned symmetry of the associated vibrational modes, which would predict that some lines should decrease more rapidly than others. This orientation dependence in the Raman scattering was ascribed to the known resonance enhancement in the Raman spectra of SWNT (Ref. 3) and an assumed orientation dependence of the absorption responsible for the resonance. In this Rapid Communication we report polarized reflectance and absorption spectra measured on oriented fibers of aligned SWNT, providing direct confirmation of the previously assumed polarization-dependent optical absorption. Such anisotropy in the optical absorption of nanotubes was predicted by Ajiki and Ando[4] and elaborated by Tasaki *et al.*[5] Additional calculations have recently been presented.[6,7] Birefringence was reported some time ago in studies of thin films of multiwalled tubes.[8]

Two types of aligned SWNT fibers were studied. One was generated by a method involving the electrophoretic attraction of the nanotubes suspended in dimethylformamide (DMF) to a positively charged 8 μm diameter carbon fiber (CF). The SWNT aggregate about this electrode forming an extended network of nanotubes attached to the electrode and to each other. Upon slow withdrawal of the CF from the solution, a free-standing fiber of SWNT (attached on one end to the CF) is drawn from the network remaining in the solution.[1] The resulting SWNT fibers have diameters of typically 2–10 μm, lengths up to several centimeters, and moderate alignment of the nanotubes along the fiber axis. The alignment was qualitatively verified by SEM, TEM, selected area electron diffraction and quantified as described below by polarized Raman spectroscopy. The second type of aligned SWNT fiber studied was a melt-spun composite fiber of 1 wt.% SWNT in polymethylmethacrylate (PMMA).[2] These fibers have diameters in the tens of μm and the very high draw ratio available in the melt-spinning process imparts exceptional alignment to the SWNT along the fiber axis.

We measured the reflectivity of the free-standing fiber and the transmission of the 1 wt.% SWNT in PMMA using a Zeiss MPM-800 microscope photometer equipped with polarizer and analyzer over wavelengths of 800–400 nm (1.5–3 eV or 12 000–25 000 cm^{-1}). For reflectance the measurement aperture in the plane of the sample was 50 $\times 50$ μm. However, the sample underfilled the aperture so the effective area was of order 10×50 μm. To measure the polarization parallel and perpendicular to the fiber axis, we kept the polarizer/analyzer fixed and rotated the specimen.

The spot size for the transmission measurement of 1 wt.% SWNT in PMMA (on a 27 μm-diameter fiber) was about 9×45 μm; in this case lensing in the circular cross-section fiber only allowed light to escape from the central third of the surface. This lensing effect substantially reduced the apparent transmission. Attempts to compensate for the lensing by using a pure PMMA fiber were only partially successful, probably on account of small differences in size and shape among the fibers.

In addition, we measured the absolute reflectance of an unoriented SWNT free-standing film over a wide wavelength range, using techniques described previously.[9] The data extend from the far infrared (15 cm^{-1} or 2 meV) to the ultraviolet (40 000 cm^{-1} or 5 eV). The reflectance is corrected (to first approximation) for the scattering from the rough surface of the sample by overcoating with a thin layer of gold, measuring the reflectance of the gold-coated surface, calculating the ratio of the reflectance of the uncoated to coated sample, and multiplying by the (known) reflectance of gold.

The degree of SWNT alignment in the two types of fibers studied was determined by polarized Raman spectroscopy using 647.1 nm excitation. For the VV measurement geometry the Raman intensity of an oriented SWNT is proportional to $\cos^4\theta$ where θ is the angle between the SWNT axis (in the plane perpendicular to the Poynting vector of the incident excitation) and the incident excitation polarization.[1] For a fiber comprised of SWNT distributed over a range of angles the total Raman intensity can be integrated to sum the contribution from nanotubes at each angle. Thus, the intensity of a Raman peak may be written as

$$I(\Psi) = \int_{\Psi - \pi/2}^{\Psi + \pi/2} cF(\theta - \Psi, \Delta) \cos^4\theta \, d\theta, \qquad (1)$$

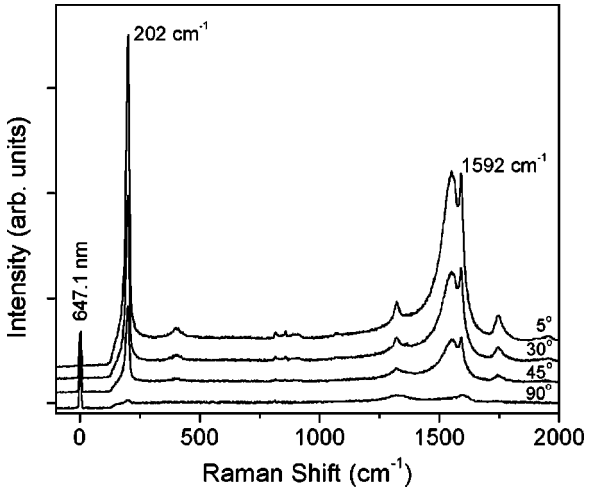

FIG. 1. Polarized Raman spectra of 1 wt.% SWNT in a melt-spun PMMA fiber. Spectra are recorded with the analyzer axis parallel to the polarization axis of the 647.1 nm excitation. Each curve is the spectrum for the indicated fiber orientation with respect to the incident polarization. (The fiber rotations are in the plane perpendicular to the Poynting vector of the excitation.)

where Ψ is the fiber angle with respect to the incident polarization, $F(\theta-\Psi,\Delta)$ is a distribution function of angular width characterized by the parameter Δ, and c is a parameter that gives the maximum intensity when $\theta=0$. The degree of SWNT alignment is determined by measuring $I(\Psi)$ for a convenient Raman peak at several fiber angles and performing a least squares fit to Eq. (1) (adjusting c and Δ to minimize the variance). The choice of distribution function is left to that which fits the data best. We have found a Lorentzian form to work well, i.e.,

$$F(\theta-\Psi,\Delta)=\frac{\Delta/2\pi}{(\theta-\Psi)^2-(\Delta/2)^2}, \tag{2}$$

where Δ is the full width at half maximum (FWHM) of the distribution.

In Fig. 1 we show the Raman spectra at several fiber angles for a melt-spun composite fiber (1 wt.% SWNT). The decrease in intensity with increasing angle between the fiber axis and polarization direction is very evident.

Figure 2(a) plots the 202 cm^{-1}, breathing-mode peak intensity as a function of fiber angle. To account for local variations in SWNT alignment, several spectra were recorded at each fiber angle following a small translation of the excitation beam along the fiber axis. Also shown in Fig. 2 is the resulting fit of Eq. (1) to the data using the best-fit parameters for c and Δ. The fit gives a FWHM of 4° for the angular distribution. This is compared to a simple $\cos^4\Psi$ (dashed line) expected for perfect alignment. Melt-spinning can yield remarkably well-aligned SWNT fibers. Figure 2(b) plots the breathing mode intensity vs fiber angle for a smaller draw ratio melt-spun fiber which results in less well aligned SWNT (fitted FWHM, $\Delta=16°$). The better aligned of these melt-spun fibers was used in the optical transmission measurements described below. Aligned fibers made by drawing from the DMF solution give significantly worse alignment but have the virtue of being comprised wholly of SWNT. Because they are opaque to optical radiation these fibers

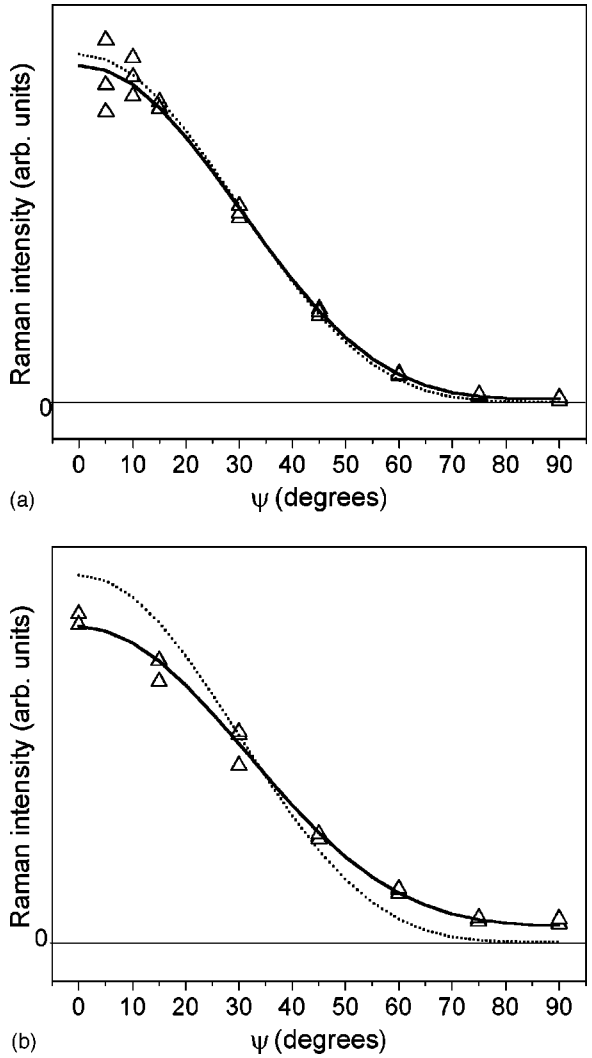

FIG. 2. Measured breathing mode peak intensity (202 cm^{-1}) as a function of fiber angle Ψ (triangles) for a 1 wt.% SWNT in a melt-spun PMMA fiber. Solid lines are the best fit of Eq. (1) to the data giving a FWHM for the Lorentzian angular distribution spread of 4°, (a) and 16°, (b) a less well aligned fiber. The dotted lines are $\cos^4(\Psi)$, expected for the case when the SWNT are perfectly aligned along the fiber axis.

were measured in reflectance. The Raman based orientation analysis for the drawn fiber used in the reflectivity measurements gave a FWHM for the SWNT angular distribution of $\Delta=23°$.

Figure 3 shows the unpolarized reflectance of an unoriented SWNT free-standing film over the frequency range from 15 to 25 000 cm^{-1} (2 meV–3 eV). Also shown is a fit to the reflectance that uses a dielectric function model consisting of a Drude term to represent the free-carrier response, Lorentzian oscillators (locations indicated by arrows) for interband transitions, and a constant high-frequency dielectric function. These results indicate that the material consists of a mixture of conducting/small bandgap [armchair/$n\equiv m$ (mod3)] nanotubes and semiconducting [$n\not\equiv m$ (mod3)] nanotubes. The peaks correspond to transitions between density-of-states (DOS) peaks of these tubes. Their energy locations are consistent with electronic structure calculations for 1.4 nm diameter tubes[4,5,10,11] as well as with

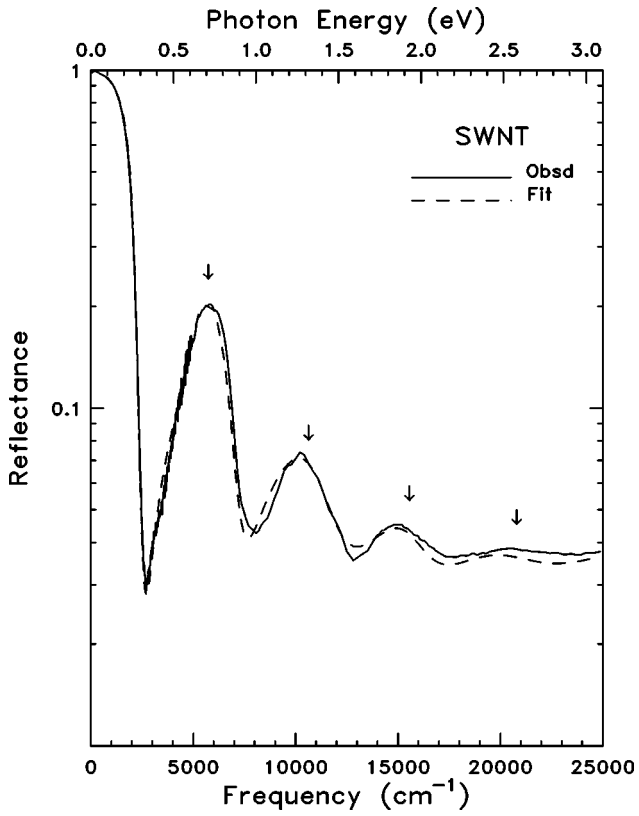

FIG. 3. Reflectance of an unaligned mat of single-wall carbon nanotubes over 25–25 000 cm^{-1} (lower scale) or 3 meV–3 eV (upper scale).

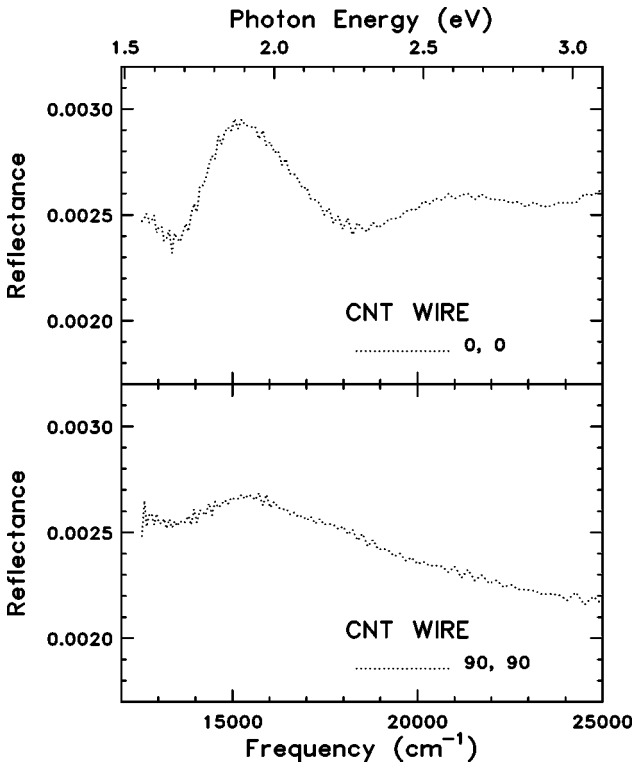

FIG. 4. Polarized reflectivity of a free-standing fiber made up of single-wall carbon nanotubes for electric field parallel (upper panel) and perpendicular (lower panel) to the fiber (and SWNT) axis.

energy-loss[12] and unpolarized optical[13] measurements on similar samples. The strong plasma edge is associated with the metallic and small bandgap SWNT. The peaks at 0.7 and 1.3 eV are assigned to transitions between the first and second pairs of DOS peaks of semiconducting tubes. The 1.9 eV and 2.6 eV bands have intensity from predominantly metallic and semiconducting tubes, respectively. Some larger diameter, semiconducting tubes may contribute to the 1.9 eV peak (the transition from the third valence to third conduction band DOS peak) and some larger diameter metallic tubes may contribute to the 2.6 eV peak with their second valence band to second conduction-band transition. However, because the diameter distributions of nanotubes in these samples is sharply peaked around 1.4 nm, such contributions are expected to be very small. The peaks at 1.9 and 2.6 eV are the features whose polarization dependence we have measured.

Figure 4 shows the polarized reflectivity of a free-standing SWNT fiber for electric field parallel (upper panel) and perpendicular (lower panel) to the fiber (and SWNT) axis. Considerable anisotropy is evident. In particular, the bands at 1.9 eV and 2.6 eV are strongly polarized in the parallel direction, although some of the more intense 1.9 eV feature appears in the perpendicular polarization due to the misaligned SWNT in the fiber. As already mentioned, the curved surface and small area of the fiber gives large systematic errors in the magnitude of the reflected signal; however, we believe that the spectral features are accurately given by these data.

Figure 5 shows the polarized absorption of a melt-spun

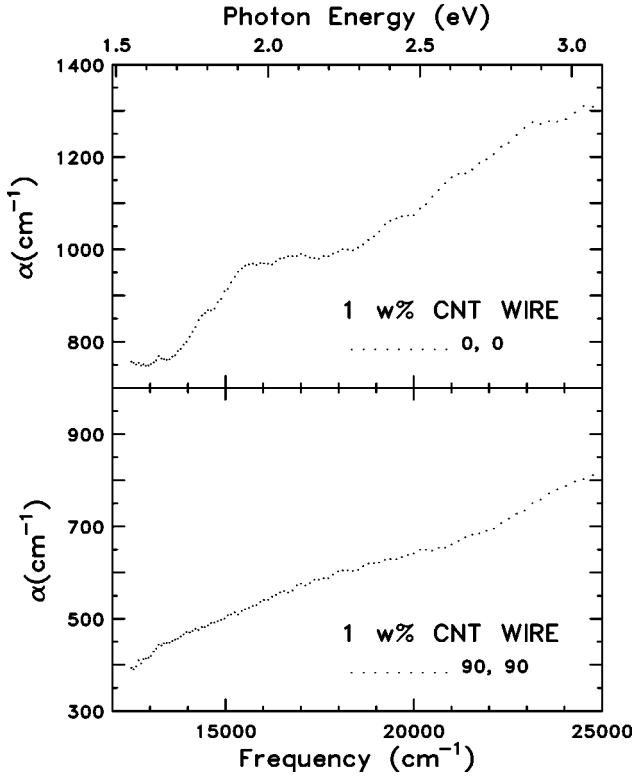

FIG. 5. Polarized absorption coefficient of a 1 wt.% single-wall carbon nanotubes in polymethylmethacrylate (PMMA) for electric field parallel (upper panel) and perpendicular (lower panel) to the fiber (and SWNT) axis.

composite fiber of 1 wt.% SWNT in PMMA for electric field parallel (upper panel) and perpendicular (lower panel) to the fiber (and SWNT) axis. The measured absorption coefficient is calculated from the reflectance, using $\alpha=(1/d)\ln T$, where d is the sample thickness and T the transmittance. We used the diameter of the fiber as the thickness in estimating the absorption coefficient. This sample is a composite of small, polarizable, absorbing entities (the SWNT) embedded at random in a weakly absorbing host (the PMMA). The effective optical response of this inhomogeneous medium is affected by local-field corrections. Because the the volume fraction f of absorbing component is small, the Maxwell-Garnett model, modified to account for the nonspherical shape of the SWNT, can be used to model the dielectric function of the composite.[14,15] The absorption coefficient is

$$\alpha=fD(\epsilon_h,\epsilon_{nt},f,g)\alpha_{nt}+(1+f/g)\alpha_h, \qquad (3)$$

where α_{nt} is the absorption coefficient of the SWNT and α_h is the absorption coefficient of the host. The factor g is a shape-dependent depolarization factor, equal to 1/3 for spheres but substantially smaller for oriented needle-shaped ellipsoids with the field parallel to the needle axis. The function $D(\epsilon_h,\epsilon_{nt},f,g)$ represents the effects of the local-field corrections and of averaging the fields and currents over the two constituents. In the case where $f\ll 1$, $f<g$, and the refractive index mismatch between host and inclusion is not large, D is close to unity. Finally, because we used a PMMA fiber as reference, the host absorption, which is small anyway, is not as big a factor in our results as the already mentioned lensing effects. Consequently, we interpret the bands in the data as due to absorption by the SWNT in the PMMA fiber.

Considerable anisotropy is evident in the data of Fig. 5. In particular, the band at 1.9 eV is strongly polarized in the parallel direction, although there is some absorption, evidently at lower energies, in the perpendicular polarization.

In conclusion we have measured by reflectance and transmittance the polarized absorption of single-walled carbon nanotubes in the 1.5–2.5 eV region of the spectrum. The two absorptions present in this region are strongly polarized along the tube axis. This result confirms the interpretation of the polarization-dependence of the Raman spectrum as due to matrix element effects in the resonant enhancement factors.

Work at the University of Florida was supported in part by the National Science Foundation through DMR-9705108. Seed funding for the work at the University of Pennsylvania was provided by the NSF MRSEC Program DMR96-32598 and USDOE Grant No. DEFG02-98ER45701.

[1] H. H. Gommans, J. W. Alldredge, H. Tashiro, J. Park, J. Magnuson, and A. G. Rinzler, J. Appl. Phys. **88**, 2509 (2000).

[2] R. Haggenmueller, H. H. Gommans, A. G. Rinzler, J. E. Fischer, and K. I. Winey, Chem. Phys. Lett. (to be published).

[3] A. M. Rao, E. Richter, S. Bandow, B. Chase, P. C. Eklund, K. A. Williams, S. Fang, K. R. Subbaswamy, M. Menon, A. Thess, R. E. Smalley, G. Dresselhaus, and M. S. Dresselhaus, Science **275**, 187 (1997).

[4] H. Ajiki and T. Ando, Physica B **201**, 349 (1994).

[5] S. Tasaki, K. Maekawa, and T. Yambe, Phys. Rev. B **57**, 9301 (1998).

[6] M. F. Lin, F. L. Shyu, and R. B. Chen, Phys. Rev. B **61**, 14 114 (2000).

[7] I. Božović, N. Božović, and M. Damnjanović, Phys. Rev. B **62**, 6971 (2000).

[8] W. A. de Heer, W. S. Bacsa, A. Chatelain, T. Gerfin, R. Humphrey-Baker, L. Forro, and D. Ugarte, Science **268**, 845 (1995).

[9] Akito Ugawa, Andrew G. Rinzler, and D. B. Tanner, Phys. Rev. B **60**, R11 305 (1999); to be published.

[10] N. Hamada, S. Sawada, and A. Oshiyama, Phys. Rev. Lett. **68**, 1579 (1992).

[11] C. L. Kane and E. J. Mele, Phys. Rev. Lett. **78**, 1932 (1997).

[12] T. Pichler, M. Knupfer, M. S. Golden, J. Fink, A. Rinzler, and R. E. Smalley, Phys. Rev. Lett. **80**, 4729 (1998).

[13] S. Kazaoui, N. Minami, R. Jacquemin, H. Kataura, and Y. Achiba, Phys. Rev. B **60**, 13 339 (1999); S. Kazaoui, N. Minami, H. Yamawaki, K. Aoki, H. Kataura, and Y. Achiba, Phys. Rev. B **62**, 1643 (2000).

[14] E. Šimánek, Phys. Rev. Lett. **38**, 1161 (1977).

[15] A review of the theories and far infrared properties of inhomogeneous media by G. L. Carr, S. Perkowitz, and D. B. Tanner may be found in *Infrared and Millimeter Waves*, Vol. 13, edited by K. Button (Academic, New York, 1985), p. 172.